phys. stat. sol. (c) **2**, No. 2, 906–909 (2005) / **DOI** 10.1002/pssc.200460337

Dynamics of relaxation and trapping of excitons in $Al_xGa_{1-x}As$ films

A. Amo[*1], **M. D. Martin**[1], **L. Klopotowski**[1], **L. Viña**[1], **A. I. Toropov**[2], and **K. S. Zhuravlev**[2]

[1] Dept. Física de Materiales, Universidad Autónoma de Madrid, 28049 Madrid, Spain
[2] Institute of Semiconductor Physics, Pr. Lavrentieva, 13, 630090 Novosibirsk, Russia

Received 29 June 2004, accepted 9 July 2004
Published online 15 February 2005

PACS 71.35.–y, 78.47.+p, 78.55.Cr, 78.66.Fd

Carrier relaxation in high quality $Al_xGa_{1-x}As$ (x up to 5%) epilayers has been investigated by means of time resolved photoluminiscence. The time for the excitonic PL to reach the maximum intensity shows a non-monotonic behaviour with increasing excitation density, which is attributed to the competition between exciton localization and carrier-carrier scattering. The increase of the Al content enhances the alloy scattering and increases the number of localization sites, moderately accelerating the dynamics. A four-level rate equation model qualitatively describes the influence of trapping in the exciton dynamics at low excitation densities.

1 Introduction

The performance of semiconductor optoelectronic devices are greatly influenced by the relaxation and lifetimes of photoexcited electron-hole pairs. To optimize the speed of such devices it is important to have a precise knowledge of the response of the carriers to a short optical pulse. GaAs quantum wells (QWs) have been the subject of intense study using time-resolved spectroscopy in the last decades [1–3]. Those studies show that the energy of photoexcited carriers relaxes via emission of acoustic phonons and through exciton-exciton interaction [1]. In spite of the fact that the ternary compound $Al_xGa_{1-x}As$ is a key material to fabricate heterostructures with GaAs active layers, such as superlattices, GRINSCH, microcavities, etc, very little attention has been paid to the excitonic dynamics in this material, mainly due to the lack of high quality epilayers. To understand the relaxation processes in these complex heterostructures it is crucial to understand them in their bulk constituents.

The physical processes governing the energy relaxation of excitons in bulk GaAs have been investigated in the past by a detailed analysis of their time evolution, paying special attention to the time for the photoluminescence (PL) to reach its maximum (t_{max}). A wide dispersion in t_{max} values can be found in the literature, from ~50 ps [4] up to ~1 ns [5]. In this paper we present a systematic analysis of t_{max} in several $Al_xGa_{1-x}As$ epilayers under non-resonant excitation for various excitation densities. We will show that t_{max} can be significantly influenced by the trapping of excitons, leading to a non-monotonic behaviour in the dependence of t_{max} with excitation density. Furthermore, we will demonstrate that the time profiles are altered by the presence of localization centers.

2 Sample description and experimental setup

Four high quality $Al_xGa_{1-x}As$ epilayers of 2.5 μm thickness, with Al concentration x=0, 1.5%, 3% and 5%, grown by Molecular Beam Epitaxy have been investigated [6]. All the samples, which were nomi-

[*] Corresponding author: e-mail: alberto.amo@uam.es, Phone: +34 914 974 771, Fax: +34 914 978 579

nally undoped, showed *p*-type conductivity, with hole concentrations ranging between 1-8x10^{14} cm^{-3}. The samples are mounted in a cold finger cryostat, and all the measurements are performed at a temperature of 5 K. The optical excitation source is an Ar^{+}-pumped Ti:Shappire laser with 2 ps long pulses and a repetition rate of 82 MHz. The PL, excited non-resonantly, is dispersed by a 60 cm spectrograph and time-resolved by a synchroscan streak camera. The overall time resolution of the system is below 12 ps and the energy resolution better than 0.2 meV. Low temperature characterization of the samples by cw photoluminescence excitation (not shown here) allows a precise identification of the free and bound exciton peaks (FX and BX, respectively) [7]. Despite the existence of emission from localized states, the narrowness of the lines at low excitation densities assures the good quality of the samples.

3 Results

Figure 1 shows the PL spectra of the GaAs sample for low and high excitation densities. At low excitation densities (solid line), band-to-acceptor –e^{-}-A^{0}– and acceptor BX states –A^{0}-X, (A^{0}-X)*–, related to carbon impurities [6], as well as FX luminescence can be clearly seen. At higher densities (dashed line), the emission from the FX overcomes that of the BX, due to the filling of the finite number of localized states. Concomitantly, the FX energy redshifts with increasing density as a consequence of the change in binding energy and bandgap renormalization caused by the many body carrier-carrier interactions that take place at high excitation powers [8].

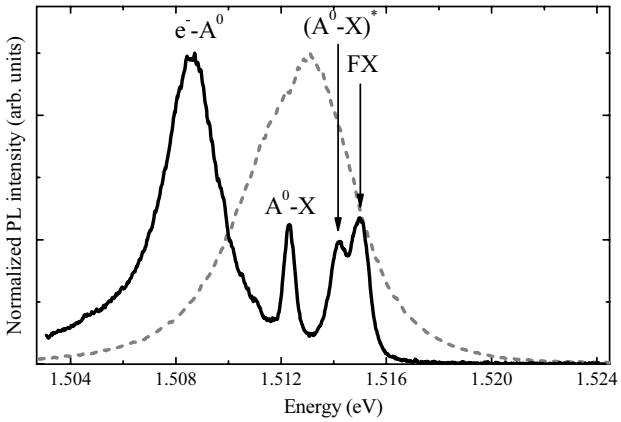

Fig. 1 Low temperature PL spectra of the GaAs epilayer recorded at a delay of 2 ns at excitation densities of 2x10^{14} cm^{-3} (solid line) and 1x10^{17} cm^{-3} (dashed line) and excitation energy 1.630 eV.

Figure 2a shows the time evolution of the FX and the A^{0}-X emission in GaAs. t_{max} can be easily assigned, as depicted in the figure for the FX. The characteristic values of t_{max} are in the range of 1 ns, in agreement with previously reported values for high-quality GaAs epilayers [5].

Figure 3a depicts the dependence of t_{max} on carrier density (n) for the $Al_xGa_{1-x}As$ epilayers investigated. All the layers show a similar non-monotonic behaviour, with a maximum t_{max} at a carrier density n~1.2x10^{16} cm^{-3} = n_{x-x}. This density corresponds to a mean distance between excitons of ~40 nm. This distance is of the same order of magnitude as the exciton Bohr radius (a_B) in GaAs (11.2 nm). Hence, for $n>n_{x-x}$, exciton-exciton scattering will lead to the relaxation of excitons towards states with centre of mass momentum K~0. This mechanism reduces t_{max} significantly, as has been previously reported in QWs [1, 9]. The threshold density n_{x-x} depends on a_B only and thus is independent of the Al content for low concentrations. For $n<n_{x-x}$, t_{max} shows a steady increase with increasing carrier density. This behaviour can be understood considering the trapping of FX with K~0 into localized states. The PL spectra in this regime show the emission of both BX and FX (Fig. 1, solid line). We have also observed that t_{max} is longer for the BX than for the FX (Fig. 2a), revealing longer energy relaxation processes in the case of BX. Additionally, at short times after excitation, the PL evolution of the BX is concave, while that of the FX is convex. The concave curvature of the BX traces indicates that the build up of the BX population results from a multi-step relaxation process. All these facts evidence that the source of the BX lumines-

cence is the trapping of FX with K~0, in a cascade process similar to that observed when carriers from the barrier are trapped in quantum dots [4, 10].

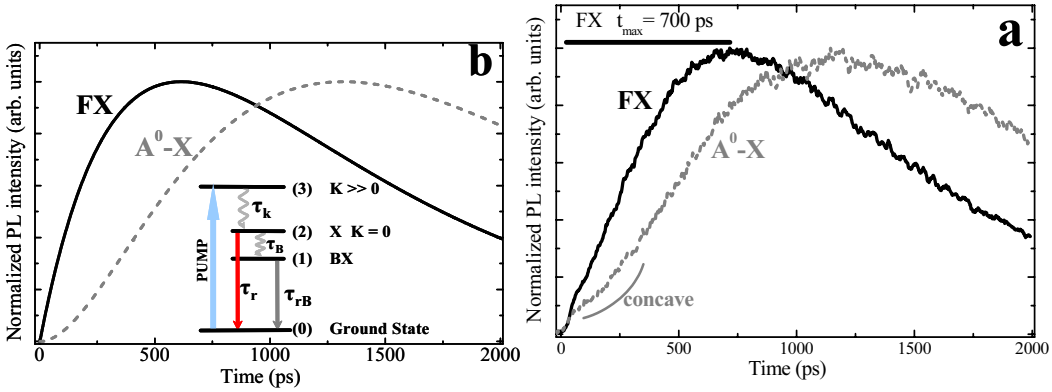

Fig. 2 (a) Time evolution of the FX (solid line) and the BX (A^0-X; dashed line) for the GaAs sample for an excitation density of $7.5x10^{14}$ cm^{-3} and excitation energy 1.563 eV. (b) Time evolution of the FX (solid line) and the BX (dashed line) extracted from the four level model described in the text. The inset shows the level scheme and the transitions considered in the model.

To account for this cascade process we have considered a four-level rate equation model, which is depicted in the inset of Fig. 2b. The pump pulse creates electron-hole pairs, which rapidly form excitons with large K (level 3). Then, excitons relax towards the radiative states with K~0 (level 2), via emission of acoustic phonons [5]. This is the conventionally considered energy relaxation step, characterized by τ_k. From these states the FX may either radiatively recombine (τ_r) or get trapped (τ_B) giving rise to a BX population (level 1), which can also radiatively recombine (τ_{rB}). The rate equations derived from this model can be easily solved analytically. Figure 2b shows the time evolution traces for the FX and the BX extracted from the model for typical times: τ_k = 800 ps, τ_B = 900 ps, $\tau_r = \tau_{rB}$ = 1000 ps. A comparison of the two panels in Fig. 2 shows the good agreement between the simulations and the experiments: the main features of the experimental traces are reproduced, including the concave curvature of the BX time evolution at short times after excitation.

The model accounts also for the carrier density dependence of t_{max} at low powers depicted in Fig. 3a. The number of trapping states is finite (of the order of the residual hole density $1\text{-}8x10^{14}$ cm^{-3}) and these states are gradually filled when the excitation density is increased. When the excitation density is high enough, the number of localization sites is small compared to the FX population, and the trapping channel can be neglected in the dynamics of the exciton population. This situation can be described by the model eliminating the BX level. Keeping the same values of τ_k (800 ps) and τ_r (1000 ps) and taking $\tau_B \rightarrow \infty$, the model gives a t_{max} considerably longer –900 ps– than that obtained in the presence of the localization channel –615 ps– (↑, ↓ in Fig. 3b). This is in qualitative agreement with the increase of t_{max} with carrier density shown in Fig. 3a.

The main effects of raising the Al content in the samples are an enhancement of the alloy scattering and an increase in the number of localization traps. This increase results in a reduction of the trapping time τ_B [11] and therefore a decrease of t_{max}, as borne out by our experiments. The influence of τ_B on the dynamics of the FX is summarized in Fig. 3b, which displays the computed FX time evolution for different τ_B's using the above mentioned values of τ_k, τ_r and τ_{rB}. The solid line corresponds to no trapping ($\tau_B \rightarrow \infty$), modelling the case when all the localized states are occupied ($n > n_{x-x}$). For $n < n_{x-x}$ (shaded box in Fig. 3a), the reduction of t_{max} with increasing Al content, due to the increase of the localization sites, is reproduced by the model by reducing τ_B (Fig. 3b), i.e. higher localization probability. For a 5% of Al the trapping time is reduced by a factor of ~20.

This simple phenomenological model can account for the dispersion in t_{max} values found in the literature in GaAs epilayers. Shen *et al.* [4] find a value of t_{max} for the FX at 2 K of ~50 ps, which is almost

independent of the excitation density. This result can be well reproduced by our four level model if τ_B is very short compared to τ_k. Indeed their PL spectra are dominated by the BX emission at all excitation powers, evidencing a high density of localization sites.

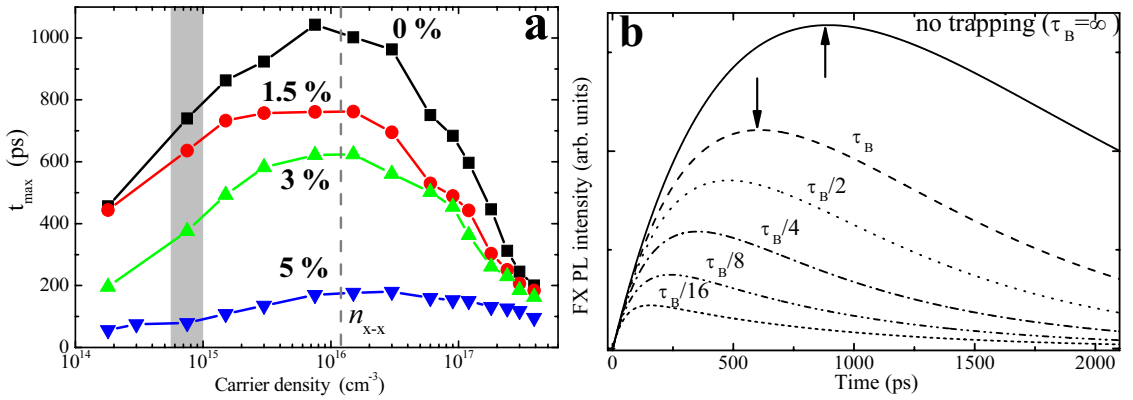

Fig. 3 (a) Measured t_{max} as a function of excitation density for the FX in the four investigated $Al_xGa_{1-x}As$ epilayers (b) Simulated FX time evolution for different values of τ_B.↑ (↓) indicate t_{max} for $\tau_B = \infty$ (900 ps) and for the carrier densities highlighted by the shaded box.

4 Conclusions

We have studied the relaxation, trapping and recombination dynamics of excitons in high quality $Al_xGa_{1-x}As$ ($x \leq 5\%$) epilayers. We have observed that the time to reach the maximum emission intensity displays a non-monotonic behaviour with excitation power. We have found two different regimes in the relaxation dynamics delimited by the exciton density for which the distance between excitons and their size becomes comparable (n_{x-x}). Below this density, the relaxation is governed by the trapping of FX into BX. Above n_{x-x} exciton-exciton scattering is the predominant mechanism. We have proposed a four-level rate equation model that can qualitatively account for the different responses to changing the excitation density and the Al content.

Acknowledgements This work was partially supported by the Spanish MCYT (MAT2002-00139), the CAM (GR/MAT/0099/2004) and the network "Marie-Curie: Physics of Microcavities" (MRTN-CT-2003-503677). A. A. acknowledges a fellowship of Spanish Secretaría de Estado de Educación y Universidades (MEC).

References

[1] T. C. Damen, J. Shah, D. Y. Oberli, D. S. Chemla, J. E. Cunningham, and J. M. Kuo, Phys. Rev. B **42**, 7434 (1990).
[2] J. Martinez–Pastor, A. Vinattieri, L. Carraresi, M. Colocci, P. Roussignol, and G. Weimann, Phys. Rev. B **47**, 10456 (1993).
[3] H. W. Yoon, D. R. Wake, and J. P. Wolfe, Phys. Rev. B **54**, 2763 (1996).
[4] J. X. Shen, R. Pittini, Y. Oka, and E. Kurtz, Phys. Rev. B **61**, 2765 (2000).
[5] M. Gurioli, P. Borri, M. Colocci, M. Gulia, F. Rossi, E. Molinari, P. E. Selbmann, and P. Lugli, Phys. Rev. B **58**, R13403 (1998).
[6] K. S. Zhuravlev, A. I. Toropov, T. S. Shamirzaev, and A. K. Bakarov, Appl. Phys. Lett. **76**, 1131 (2000).
[7] U. Heim and P. Hiesinger, phys. stat. sol. (b) **66**, 461 (1974).
[8] S. Schmitt–Rink, D. S. Chemla, and D. A. B. Miller, Phys. Rev. B **32**, 6601 (1985).
[9] P. Roussignol, C. Delalande, A. Vinattieri, L. Carraresi, and M. Colocci, Phys. Rev. B **45**, 6965 (1992).
[10] F. Adler, M. Geiger, A. Bauknecht, F. Scholz, H. Schweizer, M. H. Pilkuhn, B. Ohnesorge, and A. Forchel, J. Appl. Phys. **80**, 4019 (1996).
[11] D. Bimberg, H. Münzel, A. Steckenborn, and J. Christen, Phys. Rev. B **31**, 7788 (1985).